Tribological Behavior of PolyJet-Manufactured Digital ABS Plus under Dry and Boundary Lubricated Abrasive Wear

PETER PANEV, MIGLENA PANEVA
Institute of Information and Communication Technologies
Bulgarian Academy of Sciences
Acad. G. Bonchev str., Block 2, 1113, Sofia
BULGARIA

Abstract: - The increasing application of PolyJet additive manufacturing for the production of functional polymer components requires comprehensive evaluation of their tribological performance under different operating conditions. The limited information of a wear behavior under abrasive loading requires its observation. The present study investigates the abrasive wear resistance of Digital ABS Plus specimens manufactured by PolyJet technology in the XY build orientation under dry friction and boundary lubrication conditions. Cylindrical specimens were fabricated using an Objet260 Connex 3 system and tested on a pin-on-disc tribometer against a fixed corundum abrasive surface. The experiments were performed at four normal loads (4.5, 9.0, 13.2 and 18.0 N) and four sliding distances corresponding to 100, 200, 400 and 600 friction cycles. Mass wear, wear rate, linear wear, wear intensity and wear resistance were determined and comparatively analyzed for both friction regimes. Regression analysis and phenomenological wear model were expressed and analyzed according to performed experiments. The obtained results demonstrate a pronounced nonlinear wear behavior typical of photopolymer materials. Under low normal loads, boundary lubrication significantly improves the wear resistance compared with dry friction, whereas at higher loads the protective lubricating film becomes less effective, resulting in accelerated wear.

Key-Words: - PolyJet printing, tribology, dry friction, boundary lubrication, orientation of printing, wear resistance

Received: April 5, 2026. Revised: August 9, 2026. Accepted: September 6, 2026. Available online: November 27, 2026.

1 Introduction

In recent years, additive manufacturing has been increasingly applied in mechanical engineering, the automotive industry, medicine, and tooling because it enables the production of components with complex geometries, high accuracy, and minimal material consumption [1]. Among the various additive manufacturing technologies, PolyJet (Material Jetting) stands out for its ability to produce parts with high dimensional accuracy, low surface roughness, and good mechanical properties through the layer-by-layer ultraviolet curing of photopolymer materials [2].

One of the most widely used engineering materials in PolyJet technology is Digital ABS Plus, a photopolymer composite developed to simulate the properties of conventional ABS [3]. The material exhibits good strength, impact resistance, dimensional stability, and relatively high thermal resistance, making it suitable for functional prototypes, tooling, and structural components subjected to moderate mechanical loads. Despite its widespread use, information on its tribological behavior under actual operating conditions remains limited.

During the operation of polymer components, friction and wear processes have a substantial effect on their reliability and service life [4], [5]. Wear is the gradual degradation and removal of material from contacting surfaces as a result of their mechanical interaction. The intensity of this process depends on several factors, including the applied load, sliding speed, surface quality, build orientation in additive manufacturing, and friction regime. As a process accompanying friction, wear leads to losses of material and human resources. It is responsible for the withdrawal from service of more than 80% of components and machines as a whole [6].

Under dry-friction conditions, no separating lubricating film is present between the contacting surfaces. This results in direct interaction between surface asperities, increased local contact stresses, and intensive adhesive and abrasive wear [7], [8]. Under boundary-friction conditions, a thin lubricant

layer forms between the surfaces, reducing direct contact and limiting wear intensity [9]. The effectiveness of this protective layer depends on its stability, the contact load, and the operating conditions [10]. Consequently, the friction regime is one of the key factors governing the in-service wear resistance of polymer materials.

Studies published to date on materials produced by PolyJet technology have focused primarily on determining their mechanical properties and the influence of process parameters on the quality of printed parts [11], [12], [13]. Research addressing the tribological behavior of Digital ABS Plus, particularly under conditions close to actual service, is considerably more limited. In addition to the test parameters, the tribological characteristics are also affected by the build orientation of the part, because it determines the material's internal structure, the quality of the surface layer, and the distribution of residual stresses [14]. In practice, the XY-plane orientation is one of the most frequently used for functional parts manufactured by PolyJet technology because of its good dimensional accuracy and surface quality [15].

The aim of the present study is to analyze the wear resistance of Digital ABS Plus specimens manufactured by PolyJet technology in the XY-plane orientation by experimentally determining their tribological behavior under different operating conditions and loads. The results will contribute to a better understanding of the wear mechanisms of this class of photopolymer materials and support their selection in the development of functional engineering components. The obtained results will expand the available data on the material's tribological properties [14], [16].

2 Materials and methods

2.1 Material characteristics and specimen preparation

The present study used Digital ABS Plus, a two-component composite photopolymer supplied as a liquid resin and consisting of RGD515S (base component) and RGD531 (curing component). Table 1 presents selected physical and mechanical properties of the investigated Digital ABS Plus polymer, according to its technical data sheet.

The specimens are cylindrical, with a diameter of 10 mm and a length of 15 mm. The CAD model was imported into GrabCAD Print, version 1.115, to configure the printing parameters. Ninety-six specimens were manufactured in the XY orientation using an Objet 260 Connex 3 PolyJet 3D printer. During printing, SUP705B support material was used in matte mode, meaning that the entire part was covered with support material to ensure uniform strength. The printing layer thickness was 30 μm. After printing, the support material was removed using a WaterJet system with high-pressure water. Before testing, the specimens were left to dry horizontally for 24 h.

2.2 Wear resistance test methodology

Wear resistance was investigated by subjecting the specimens to abrasive wear at different loads—4.5, 9.0, 13.2, and 18.0 N—and for different numbers of cycles—100, 200, 400, and 600 [17].

Investigation of the abrasive wear is processed with a tribotester operating according to the pin-on-disc kinematic configuration, whose functional diagram is shown in Figure 1. The test specimen was fixed in the holder of the loading head so that its end face formed planar contact with the abrasive surface [18].

Table 1. Physical-mechanical characteristics of digital abs plus composite polymer

Parameter	**Value**
ASTM	D-638
Tensile Strength	55-60 MPa
Modulus of Elasticity	2.600-3.000 MPa
Elongation on Break	25-40%
Shore Hardness (D)	85-87 Scale D
Rockwell Hardness	67-69 Scale M
HDT, ^{0} C 0.45 MPA	45-50 ^{0} C
Density	1.18 g/cm^3

Source: created by the authors.

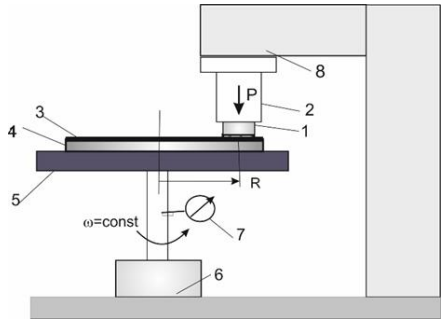

Fig. 1: Schematic diagram of the pin-on-disc tribotester used to investigate abrasive wear
Source: created by the authors.

The abrasive surface was rigidly mounted on a horizontal disc and was represented by impregnated P2000 corundum with a hardness of 9.0 on the Mohs scale. This satisfies the standard requirement that the abrasive hardness be at least 60% greater than that of

the tested material. The disc was driven by an electric motor and rotated about its central vertical axis at a constant sliding speed of $\omega=const$ (67 cm/s). The normal load P in the tribosystem was applied by means of a lever mechanism to ensure a uniform distribution of contact pressure over the contact area between the specimen and the abrasive surface.

The sliding distance S for a given number of cycles N was calculated using the:

$$S=2\pi.R.N \quad (1)$$

The sliding distance S was expressed in terms of the number of cycles (N), which were set and recorded using the revolution counter [19]. The device allows the sliding speed to be varied by changing the distance R between the center of the specimen and the center of the disc; in this study, R was 32 mm. The tests were performed at an ambient air temperature of 22 °C.

Figure 2 shows a schematic diagram of the Digital ABS Plus polymer–abrasive surface tribosystem. The build layers were oriented parallel to the relative sliding-velocity vector (longitudinal layers), and the specimens were designated Digital ABS Plus-x.

The test methodology consisted of measuring the mass wear of a specimen over a specified sliding distance (number of cycles) under constant conditions: sliding speed, load, type of abrasive surface, and ambient temperature. Mass wear (m) was determined as the difference between the initial specimen mass (before friction) and its mass after a specified sliding distance. Specimen mass was measured using a WPS 180/C/2 electronic balance with a resolution of 0.1 mg [18]. Friction, lubrication, and wear are closely related in sliding contacts [20]. Previous experiments with vegetable and mineral–vegetable oils showed that lubricant composition can affect friction [21].

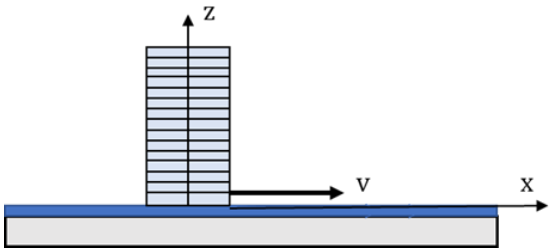

Fig. 2: Schematic diagram of the Digital ABS Plus polymer–abrasive surface tribosystem with parallel layer orientation

Source: created by the authors.

Before each measurement, the specimen was cleaned of mechanical and organic particles and wiped with ethyl alcohol to prevent electrostatic effects. A new abrasive surface was used for every specimen in each test.

After measuring the mass wear (m), the following wear characteristics were calculated: mass wear rate, linear wear, wear intensity, and wear resistance.

The mass wear rate γ is the mass removed from the specimen surface per unit friction time and is expressed in mg/s:

$$\gamma=\frac{m}{t} \quad (2)$$

The relationship between the measured mass wear m and the linear wear h of the specimen (wear normal to the sliding-velocity vector) is given by:

$$h=\frac{m}{\rho.A_a} \quad (3)$$

,where $A_a=\pi r^2$ is the nominal friction contact area, r is the radius of the contact area, and ρ is the material density at the contact location.

The abrasive wear intensity i_a is the linear wear h of the specimen per unit sliding distance S, i.e.:

$$i_a=\frac{m}{\rho.A_a.S} \quad (4)$$

The absolute wear resistance $I_r$is expressed as the reciprocal of the wear intensitym

$$I_r=\frac{1}{i_a}=\frac{\rho.A_a.S}{m} \quad (5)$$

Wear intensity and wear resistance are dimensionless quantities.

Equations (1), (2), (3), (4), and (5) were used to calculate the wear characteristics of Digital ABS Plus.

3 Experimental results, relationships, and analysis

Using the apparatus and methodology described above, experimental results were obtained for the abrasive wear characteristics—mass wear, mass wear rate, linear wear, wear intensity, and wear resistance—of Digital ABS Plus-x specimens under dry friction and boundary friction with SAE 15W-40 oil lubrication. Tests were conducted at normal loads of 4.5, 9.0, 13.2, and 18.0 N and at sliding distances corresponding to 100, 200, 400, and 600 cycles. A total of 96 experiments were performed, corresponding to 32 combinations of friction regime,

normal load, and sliding distance, with three repetitions for each condition.

The experimental data were used to plot wear kinetic curves, wear-rate relationships, and wear-resistance diagrams for Digital ABS Plus-x under both friction regimes and at all normal loads. In tribology, a "wear kinetic curve" describes the dependence of mass (or linear) wear on sliding distance (friction time or number of friction cycles) [22]. Figure 3 and Figure 4 present the mass-wear kinetic curves at four normal loads under dry-friction and boundary-friction conditions, respectively.

Under dry friction, the relationship between wear and sliding distance was nonlinear at every load. Under boundary friction at the lower loads of P = 4.5 N and P = 9.0 N, the relationship was linear and resembled the wear behavior of metals [23]. Figure 5–8 graphically present the mass wear as a function of sliding distance and the corresponding mathematical models for each load under the two friction regimes: dry and boundary friction.

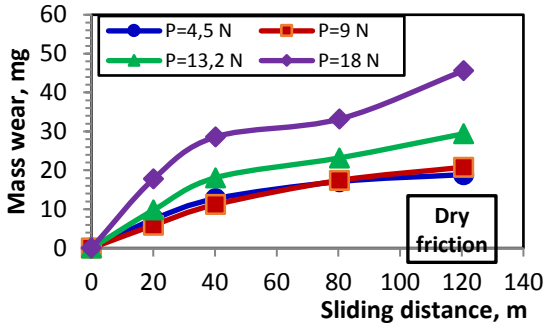

Fig. 3: Mass wear as a function of sliding distance for Digital ABS Plus-x at different normal loads under dry-friction conditions
Source: created by the authors.

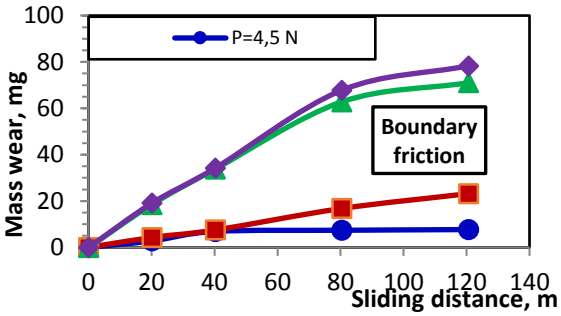

Fig. 4: Mass wear as a function of sliding distance for Digital ABS Plus-x at different normal loads under boundary-friction conditions
Source: created by the authors.

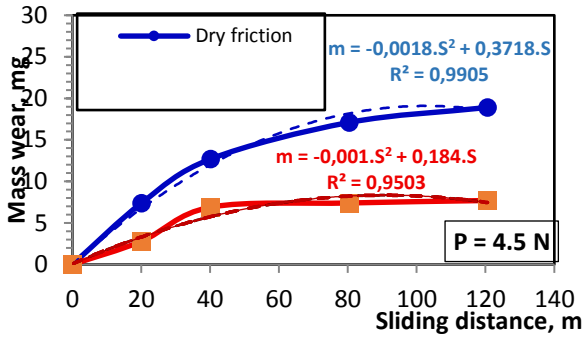

Fig. 5: Mass wear as a function of sliding distance for Digital ABS Plus-x under dry and boundary-friction conditions at a normal load of P = 4.5 N
Source: created by the authors.

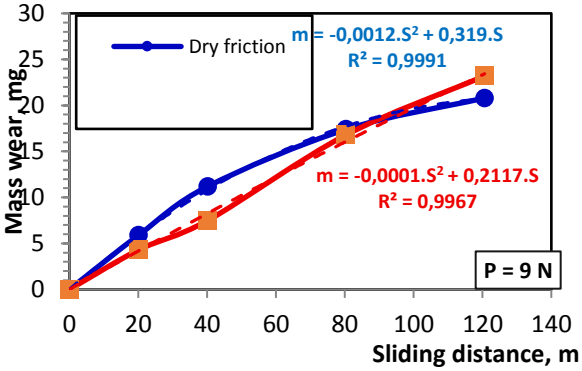

Fig. 6: Mass wear as a function of sliding distance for Digital ABS Plus-x under dry and boundary-friction conditions at a normal load of P = 9 N
Source: created by the authors.

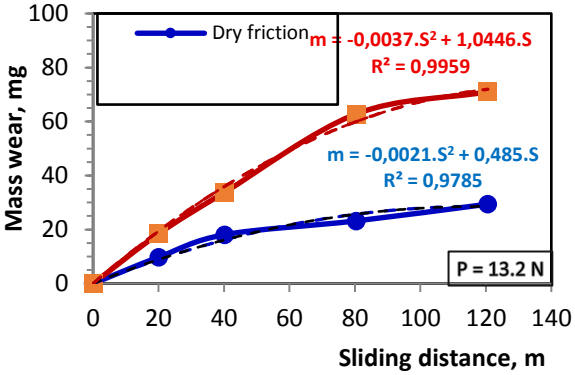

Fig. 7: Mass wear as a function of sliding distance for Digital ABS Plus-x under dry and boundary-friction conditions at a normal load of P = 13.2 N
Source: created by the authors.

At the lower loads of P = 4.5 N and P = 9.0 N, wear under dry friction was greater than under boundary friction, and the models were represented by second-order regression equations (Figure 5 and Figure 6).

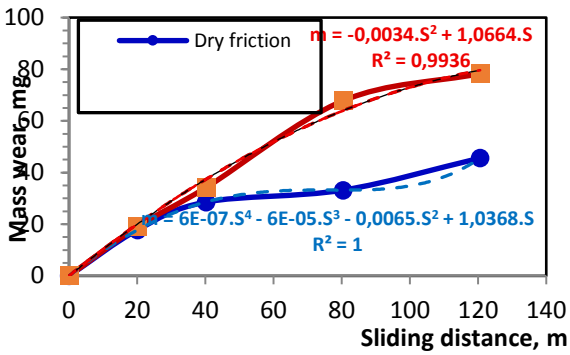

Fig. 8: Mass wear as a function of sliding distance for Digital ABS Plus-x under dry and boundary-friction conditions at a normal load of P = 18.0 N
Source: created by the authors.

At the higher normal loads, wear under boundary friction was appreciably greater than under dry friction (Figure 7 and Figure 8).

The nonlinearity of the wear kinetic curves is also reflected and confirmed by the variation in wear rate with time (Figure 9 and Figure 10).

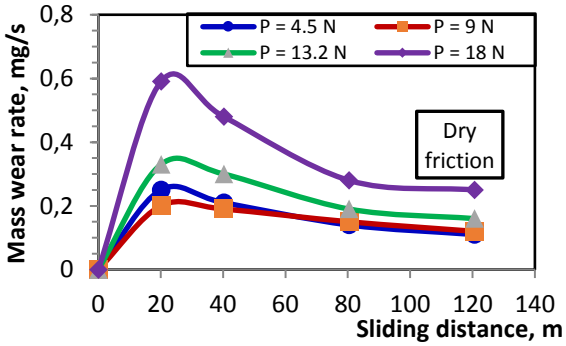

Fig. 9: Mass wear rate as a function of sliding distance for Digital ABS Plus-x at different normal loads under dry-friction conditions
Source: created by the authors.

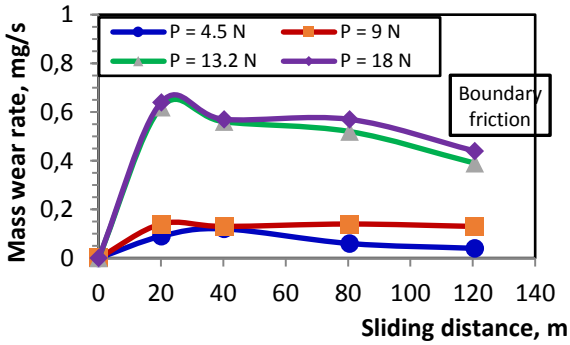

Fig. 10: Mass wear rate as a function of sliding distance for Digital ABS Plus-x at different normal loads under boundary-friction conditions
Source: created by the authors.

The wear rate did not remain constant over time (sliding distance) but decreased with varying degrees of nonlinearity depending on the load.

The pronounced nonlinearity of wear, i.e., its non-steady-state nature, is typical of polymer materials. Polymer wear mechanisms, the duration of the running-in period, and the magnitude and intensity of wear are governed by a complex set of factors that act together and, in many cases, influence one another. The principal factors include the nature and structure of the polymer molecular chains; the orientation of the build layers relative to the sliding-velocity vector; the mechanical properties of the polymer surface layer, including microhardness, elastic modulus, and Young's modulus; the geometric and physical-mechanical properties of the abrasive surface, including abrasive-particle size, shape, density, and hardness; the magnitude of the normal load; the magnitude and direction of the sliding velocity; the presence or absence of a lubricant; its chemical composition and physicochemical properties; and the kinematic configuration of the tribosystem. These factors determine the penetration depth of the abrasive particles into the polymer, the shape and number of contact spots, the actual contact area and its variation over time, the temperature, and the degree of mechanical and chemical rupture and destruction of adhesive and cohesive bonds within the polymer. All these processes evolve over time with different characteristics and intensities.

Figure 11 presents a wear-resistance diagram for Digital ABS Plus-x under dry and boundary-friction conditions at different loads and the same sliding distance of 120.6 m.

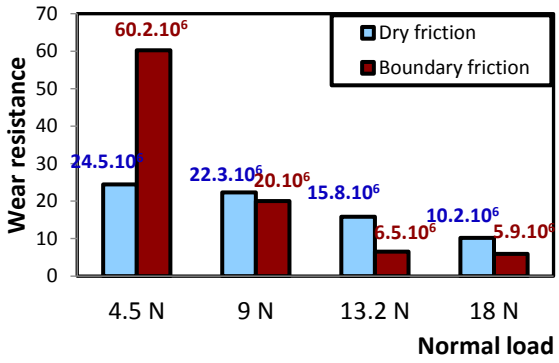

Fig. 11: Wear resistance of Digital ABS Plus-x under dry- and boundary-friction conditions at different normal loads for a sliding distance of 120.6 m
Source: created by the authors.

The highest wear resistance, 60.2×10^6, was observed under boundary-friction conditions at the

lowest normal load, P = 4.5 N. This value was approximately 2.5 times higher than that obtained under dry friction at the same load.

The lowest wear resistance of Digital ABS Plus-x, 5.9×10^6 , was observed under boundary-friction conditions at the highest load, P = 18.0 N.

In other words, the effect of load can be summarized as follows: under boundary-friction conditions, a 4.5 fold increase in the normal load resulted in a tenfold decrease in wear resistance. The relationship between wear resistance and load was strongly nonlinear. We assume that the wear mechanisms at high loads are complex: mechanical factors do not act alone; rather, tribomechanical and tribochemical processes occur simultaneously.

4 Dimensionless analysis and phenomenological wear model

The trend lines in Figure 5, Figure 6, Figure 7 and Figure 8 were re-evaluated using ordinary least-squares regression with equal weights. For all the curves, the fitted expression was:

$$M = b_1 S + b_2 S^2, \quad (6)$$

,where M is the mass loss in mg and S is the sliding distance in m; b_1 and b_2 are regression coefficients determined from the experimental data: The free term is fixed at zero, i.e. the condition M(0)=0 is imposed. Consequently, the values displayed on the figures are uncentered coefficients of determination, R_0^2, which ranged from 0.986 to 0.999 and were higher than the conventional centered values (0.853-0.998). The corresponding Root Mean Square Error (RMSE) values were 0.253-2.636 mg.

The linear coefficient was significant for all quadratic fits ($p < 0.022$). The quadratic term was significant only for dry sliding at 4.5 N ($p = 0.0196$) and 9 N ($p = 0.0050$), and for boundary lubrication at 13.2 N ($p = 0.0301$).

It was not significant for dry sliding at 13.2 N or for boundary lubrication at 4.5, 9, and 18 N ($p = 0.0605$-0.5202). Thus, the mean values do not support a statistically significant quadratic response at every load. Moreover, the negative quadratic terms can predict a decrease in cumulative wear outside the tested interval and should not be extrapolated. The fourth-order polynomial used for dry sliding at 18 N contains four coefficients for four nonzero mean values; hence, it interpolates the data exactly ($R^2 = 1$) but has zero residual degrees of freedom, so coefficient significance cannot be assessed. The legend term "Logarithmic" should therefore be replaced by "Polynomial".

A more parsimonious description was obtained by fitting all mean values within each friction regime to the following regime-dependent power law:

$$M_R(P,S) = M_{0,R} \left(\frac{P}{9}\right)^{a_R} \left(\frac{S}{40.2}\right)^{b_R}, \quad (7)$$

,where $M_R(P,S)$ is the predicted mass loss in mg given P, S and friction mode R; a_R and b_R are experimentally determined power regression coefficients, and R denotes the friction mode: D — dry, B — boundary. In Table 2 are presented the calculated coefficients.

Table 2. Regression data

Friction regime	$M_{0,R}$ (mg)	a_R	b_R	R^2	RMSE (mg)	Coefficient tests
Dry sliding	13.97	0.75	0.52	0.89	3.45	$p(a_R)$, $p(b_R) < 0.001$
Boundary lubrication	14.94	1.41	0.74	0.89	8.34	$p(a_R)$, $p(b_R) < 0.001$

Source: created by the authors.

Differentiation with respect to sliding distance gives a nonlinear wear-rate equation that includes load, distance, and friction regime:

$$\frac{dM_R}{dS} = \frac{M_{0,R} b_R}{40.2} \left(\frac{P}{9}\right)^{a_R} \left(\frac{S}{40.2}\right)^{b_R - 1} (8)$$

Numerically, the differential wear equations for the two friction regimes are:

$$\frac{dM_D}{dS} = 0.1799 \left(\frac{P}{9}\right)^{0.745} \left(\frac{S}{40.2}\right)^{-0.482} (9)$$

$$\frac{dM_B}{dS} = 0.2731 \left(\frac{P}{9}\right)^{1.406} \left(\frac{S}{40.2}\right)^{-0.265} (10)$$

The values 9 N and 40.2 m are chosen as reference values, therefore the relationships are dimensionless.

After selecting the friction mode and the specific values of P and S, the equation gives a final predicted value for the mass loss M_R in mg.

For example, for dry friction for P=18 N, S=120.6 m the dry friction model gives M_D=41.4 mg. The experimental value under these conditions is approximately 45.6 mg, i.e. the model gives a close but not exactly the same predicted value. For boundary friction under the same conditions the mass loss M_B=88.8 mg. The experimental value is approximately 78.3 mg.

Therefore, the equation gives a predicted result and not necessarily the exact experimental value. The difference between the prediction and the measurement is the residual error of the regression model.

Since $b_R < 1$, the instantaneous mass-wear rate decreases with increasing sliding distance. This behavior can be interpreted as running-in kinetics, characterized by a relatively high initial wear rate followed by gradual stabilization.

The proposed relationship can be regarded as a phenomenological extension of the classical Archard wear law [24], in which wear is proportional to the normal load and sliding distance. In the present model, however, the effective wear coefficient varies with sliding distance, allowing the transition from the running-in stage toward a quasi-steady wear regime to be represented.

The substantially higher load exponent under boundary lubrication indicates a progressive deterioration of the lubricant's protective effect as the normal load increases. The sliding-distance exponents are below unity in both regimes, which is consistent with a decreasing average wear rate after the initial running-in stage. The model is phenomenological and is valid only within the investigated ranges of P = 4.5–18.0 N and S = 20.1–120.6 m, at a sliding speed of 0.67 m/s and under the specified abrasive-contact conditions.

5 Conclusion

The principal results and findings of the present study can be summarized as follows:

A methodology was developed for measuring and determining the principal abrasive wear characteristics: mass wear, mass wear rate, linear wear, wear intensity, and wear resistance.

Experimental results were obtained for the wear characteristics described above for Digital ABS Plus-x specimens (polymer specimens whose build layers were oriented parallel to the sliding-velocity vector in the tribosystem) under two friction regimes—dry friction and boundary friction with SAE 15W-40 oil lubrication and at four normal loads.

It was established that:

the abrasive wear behavior of Digital ABS Plus is nonlinear, with different quantitative values depending on the friction regime (dry or boundary friction), the orientation of the build layers relative to the sliding-velocity vector, and the normal load;

the wear resistance of the Digital ABS Plus specimen is not constant over time; it decreases with sliding distance, and the nature of this change depends on the load magnitude and the friction regime;

the Digital ABS Plus-x specimens exhibit the highest wear resistance under boundary-friction conditions at the lowest load (P = 4.5 N);

under boundary-friction conditions, increasing the normal load by a factor of 4.5 reduces the wear resistance of the Digital ABS Plus-x specimen by a factor of 10.

Declaration of Generative AI and AI-assisted Technologies in the Writing Process

During the preparation of this work, the author(s) utilized artificial intelligence (AI) technologies solely for the purpose of linguistic refinement and grammatical correction. Following the application of these tools, the author(s) comprehensively reviewed, verified, and edited the resulting text. The author(s) maintain full accountability and responsibility for the accuracy, integrity, and final content of the publication.

References:

[1] Longfei Z., Miller J., Vezza J., Mayster M., Raffay M., Justice Q., Tamimi Z. Al, Hansotte G., Sunkara L. D., and Bernat J., Additive Manufacturing: A Comprehensive Review, Sensors 24, no. 9: 2668, April 2024 https://doi.org/10.3390/s24092668

[2] Muthuram N., Madhav P. S., Vasan D. K., Mohan M. E., Prajeeth G., A review of recent literatures in poly jet printing process, Materials Today: Proceedings, Volume 68, Part 6, pp. 1906-1920, ISSN 2214-7853, 2022, https://doi.org/10.1016/j.matpr.2022.08.090.

[3] Stratasys, PolyJetTM Materials Data Sheet [Online], Available on: https://www.stratasys.com/en/materials/materials-catalog/polyjet-materials /

[4] Raja C. P., Satyanarayana VSV., Teja P. V. S., Suresh B. V., Sridevi G., Pandipati S., Mensah RA and Babu NB K., An in-depth study on tribological behaviour of polymers and polymer composites: state-of-the-art, Front. Mater. 13:1769252, 2026, doi: 10.3389/fmats.2026.1769252

[5] Subramani R., Leon R. R., Nageswaren R., Rusho M. A., and Shankar K. V., Tribological Performance Enhancement in FDM and SLA Additive Manufacturing: Materials, Mechanisms, Surface Engineering, and Hybrid Strategies—A Holistic Review, Lubricants 13, no. 7: 298,

2025, https://doi.org/10.3390/lubricants13070298

[6] Grozdanova T., Kontaktni vzaimodeistvia v tribosistemi pri ekstremalni uslovia, Avtoreferat, Sofia, 2016; [Online], Available: https://konkursi-as.tu-sofia.bg/doks/SF_MTF/ns/330/avtoreferat.pdf; Грозданова Т., Контактни взаимодействия в трибосистеми при екстремални условия, Автореферат, София, 2016,

[7] Mitrovic Sl., Miloradovic N., Babic M., Bobic I., Stojanovic B., Dzunic D., Wear Behaviour Of Hybrid ZA27/SiC/Graphite Composites Under Dry Sliding Conditions, BulTrib, Sofia, 2012, pp. 142-147.

[8] Dangnan F., Espejo C., Liskiewicz T., Gester M., Neville A., Friction and wear of additive manufactured polymers in dry contact, Journal of Manufacturing Processes, Volume 59, pp. 238-247, ISSN 1526-6125, 2020, https://doi.org/10.1016/j.jmapro.2020.09.051 .

[9] Kotseva G., Kandeva M., Stoimenov N., and Zagorski M., Wear at Boundary Friction of 3D Printed Polymers and Composites, CODIT, pp. 473-478, 2024, 10.1109/CoDIT62066.2024.10708489.

[10] Kaya M., Tribology and the Science of Friction, Wear, and Lubrication, Macromolecules: An Indian Journal, vol. 22, no. 2, Art. 160, 2024.

[11] Dochev B., Desislava D., Zagorski M., Ublekov F., Tomanov N., and Valeva D., Investigation of the Mechanical Properties of Thermosetting Polymers Reinforced with Carbon Particles, Engineering Proceedings 100, no. 1: 21, 2025, https://doi.org/10.3390/engproc2025100021

[12] Afshar A., Mihut D., Hill S., Patrick A., Rehg Z., Norenberg M., Luo-Gardner C., and White R., Mechanical and tribological performance of molded and 3D-printed polymers under environmental degradation, Proceedings of the Institution of Mechanical Engineers, Part L: Journal of Materials: Design and Applications, 2026; 0(0). https://doi.org/10.1177/146442072614203

[13] Yosef D., ENAB T., and Eldesouky I., Tribological and hardness characteristics of resin materials in masked stereolithography: impact of washing solution and curing time, Prog Addit Manuf., Vol. 11, pp. 83–94, 2026, https://doi.org/10.1007/s40964-025-01336-6

[14] Kaur G., Singari R. M., Kumar H., A review of fused filament fabrication (FFF): Process parameters and their impact on the tribological behavior of polymers (ABS), Materials Today: Proceedings, Volume 51, Part 1, pp. 854-860, ISSN 2214-7853, 2022, https://doi.org/10.1016/j.matpr.2021.06.274.

[15] Das S. C., Ranganathan R., Murugan N., Effect of build orientation on the strength and cost of PolyJet 3D printed parts, Rapid Prototyping Journal, Vol. 24 No. 5 pp. 832–839, 2018, doi: https://doi.org/10.1108/RPJ-08-2016-0137

[16] Sontakke B. N., and Rathod V. T., Tribological Properties of PolyJet-Printed Digital Materials under Different Loading Conditions, International Journal of Scientific Research in Engineering and Management, Vol: 9, no.7, pp. 1-9 July 2025, https://doi.org/10.55041/IJSREM51271

[17] Kandeva M., Penyashki T., Kostadinov G., Kalitchin Zh., Abrasive and Erosion Wear of Composite NiCrSiB Coatings Inflicted with Subsonic Flammable Structure through a Cold Process, IOP Conference Series: Materials Science and Engineering, 724. 012014, 2020, 10.1088/1757-899X/724/1/012014.

[18] Hutchings I. M., Shipway P., Tribology: Friction and Wear of Engineering Materials. 2nd ed., Butterworth-Heinemann, Elsevier, 2017.

[19] Meng Y., Xu J., Jin Z., Prakash B., Hu Y., A review of recent advances in tribology, Friction, Vol. 8(2), pp. 221–300, 2020.

[20] Kandeva M., Kalitchin Zh., Tribological investigations of tribosystems during lubrication using vegetable oils and mineral-vegetable oil composites containing metal-plating additive. Part I: Friction, Journal of Environmental Protection and Ecology, Vol. 19. pp. 785-802, 2018

[21] Bhushan B., Introduction to Tribology. 2nd ed., John Wiley & Sons. 2013.

[22] Meng Y., Xu J., Ma L., Jin Z., Prakash B., Ma T., and Wang W., A review of advances in tribology in 2020–2021, Friction 10, pp. 1443–1595, 2022. https://doi.org/10.1007/s40544-022-0685-7

[23] Penyashki T., Kostadinov G., Kalitchin Zh., and Kandeva M., Ecological aspects of electro-spark deposition technologies for improvement of the metal surfaces quality prepared by 3d printing. Part II.

Composition, structure, durability, and environmental compliance, Journal of Environmental Protection and Ecology, Vol. 23. pp. 1483-1493, 2022.

[24] Archard J. F., Contact and Rubbing of Flat Surfaces Available to Purchase, J. Appl. Phys. 24, 981–988, 1953, https://doi.org/10.1063/1.1721448

Contribution of Individual Authors to the Creation of a Scientific Article (Ghostwriting Policy)

Peter Panev has organized and executed the experiments of Section 3.

Miglena Paneva carried out the methodology and the statistical analysis.

Sources of Funding for Research Presented in a Scientific Article or Scientific Article Itself

The research was carried out as part of project No. KP-06-M87/4 "Research the wear resistance of machine elements, possibilities for optimizing their properties through innovative methods and materials", financed by the Bulgarian National Science Fund.

Conflict of Interest

The authors have no conflicts of interest to declare that are relevant to the content of this article.

Creative Commons Attribution License 4.0 (Attribution 4.0 International, CC BY 4.0)

This article is published under the terms of the Creative Commons Attribution License 4.0
https://creativecommons.org/licenses/by/4.0/deed.en_US